PHYSICAL REVIEW A **81**, 031402(R) (2010)

Trapping ultracold atoms in a time-averaged adiabatic potential

M. Gildemeister, E. Nugent, B. E. Sherlock, M. Kubasik, B. T. Sheard, and C. J. Foot
Clarendon Laboratory, University of Oxford, Parks Road, Oxford OX1 3PU, United Kingdom
(Received 17 December 2009; published 22 March 2010)

We report an experimental realization of ultracold atoms confined in a time-averaged, adiabatic potential (TAAP). This trapping technique involves using a slowly oscillating (∼kHz) bias field to time-average the instantaneous potential given by dressing a bare magnetic potential with a high-frequency (∼MHz) magnetic field. The resultant potentials provide a convenient route to a variety of trapping geometries with tunable parameters. We demonstrate the TAAP trap in a standard time-averaged orbiting potential trap with additional Helmholtz coils for the introduction of the radio frequency dressing field. We have evaporatively cooled 5×10^4 atoms of ^{87}Rb to quantum degeneracy and observed condensate lifetimes of longer than 3 s.

DOI: 10.1103/PhysRevA.81.031402 PACS number(s): 37.10.Gh, 03.75.−b, 32.80.Xx

The use of increasingly sophisticated magnetic potentials has been crucial to the evolution of cold-atom research. The time-averaged adiabatic potential (TAAP) trap proposed in [1] combines the techniques of time-averaging and rf dressing to produce versatile potentials with a rich variety of different geometries. Since the rf dressing only couples electronic ground states of the atom, the rate of relaxation by spontaneous processes is negligible. The potential is smooth with no small-scale corrugations because the trapping region is located far from the field-generating coils. As shown in [1], the TAAP can easily sculpt complex trapping geometries such as a double-well or ring trap, which can be adiabatically modified. Here we present an experimental realization of the particular case of a double-well TAAP and an efficient way of loading it from a time-orbiting potential (TOP) trap.

The technique of time averaging involves the introduction of a time dependence to a static potential at a frequency higher than the atoms can respond to kinematically, but significantly lower than the local Larmor frequency. As a result, atoms experience a modified potential while preserving their initial m_F state. The application of a suitable rotating bias field to a quadrupole potential can circumvent Majorana losses by ensuring the field zero orbits at a radius greater than the extent of the atom cloud. For a bias field B_T rotating at angular frequency ω_T, the criterion for time averaging can be stated as $|g_F \mu_B B_T/\hbar| \gg \omega_T > \omega_r$, where g_F is the Landé g-factor, μ_B the Bohr magneton, $\hbar$ the reduced Planck constant, and ω_r the oscillation frequency of atoms in the time-averaged potential. This time-averaged, orbiting potential not only expedited the realization of a Bose-Einstein condensate (BEC) in a dilute alkali vapor [2], but also paved the way for more sophisticated magnetic potentials such as double-well [3] and ring-shaped potentials [4–6]. The general concept of using time averaging to create novel shapes of confining potentials has also been demonstrated by experiments on dipole force traps [7–9].

The repertoire of magnetic potentials was further extended by rf dressing, as proposed by Zobay and Garraway [10]. Their technique brought about the possibility of highly asymmetric two-dimensional magnetic potentials [11–13]. It has also been applied in atom chip experiments to give flexible double-well potentials [14,15] as described in detail elsewhere [10,16–18]. Radio frequency dressing involves a magnetic field oscillating at a frequency ω_{rf} comparable to the atomic Larmor frequency, which drives transitions between Zeeman sublevels in a hyperfine manifold of the atom's electronic ground state. Here the eigenstates of the system are the dressed states [19]. The variation of the corresponding eigenenergies with position gives rise to an adiabatic potential (AP) given by

$$U_{AP}(\mathbf{r}) = m_F \hbar \sqrt{\delta^2(\mathbf{r}) + \Omega_R^2(\mathbf{r})}, \tag{1}$$

where $\delta(\mathbf{r}) = |g_F \mu_B B(\mathbf{r})/\hbar| - \omega_{rf}$ is the angular frequency detuning and $\Omega_R(\mathbf{r})$ the Rabi frequency given by

$$\Omega_R(\mathbf{r}) = \left| \frac{g_F \mu_B}{2\hbar} \frac{\mathbf{B}(\mathbf{r})}{|\mathbf{B}(\mathbf{r})|} \times \mathbf{B}_{rf} \right|. \tag{2}$$

In this experiment we use a quadrupole field of the form

$$\mathbf{B}_q(\mathbf{r}) = B_q'(x\hat{\mathbf{e}}_x + y\hat{\mathbf{e}}_y - 2z\hat{\mathbf{e}}_z), \tag{3}$$

where B_q' is the radial gradient. When dressed with an rf field, $\mathbf{B}_{rf}$, the upper dressed state, has a minimum on an ellipsoidal iso-B surface where $\delta(\boldsymbol{r}) = 0$. The vectorial nature of the coupling [see Eq. (2)] gives a variation of the potential on the ellipsoidal shell itself: for linearly polarized rf with $\mathbf{B}_{rf}(t) = B_{rf}\cos(\omega_{rf}t)\hat{\mathbf{e}}_\mathbf{z}$, the coupling varies from a maximum on the equator to zero at the poles. For circularly polarized rf with $\mathbf{B}_{rf}(t) = B_{rf}[\cos(\omega_{rf}t)\hat{\mathbf{e}}_\mathbf{x} \pm \sin(\omega_{rf}t)\hat{\mathbf{e}}_\mathbf{y}]$, the coupling is a maximum at one pole and zero on the other.[1]

Radio-frequency dressed-state adiabatic potentials may themselves be time averaged to give a new class of potentials referred to as TAAPs. We have generated a double-well TAAP by applying rf radiation to a conventional TOP trap. The instantaneous potential of the TOP is a quadrupole field, which, in a TAAP trap, is dressed to give the ellipsoidal surface as described above. The oscillating bias field of the TOP trap, $\mathbf{B}_T(t) = B_T[\cos(\omega_T t)\hat{\mathbf{e}}_\mathbf{x} + \sin(\omega_T t)\hat{\mathbf{e}}_\mathbf{y}]$, causes the ellipsoidal surface to orbit in the xy plane about the axis of rotation as illustrated in Fig. 1. When $\omega_{rf} > |g_F \mu_B B_T/\hbar|$, the ellipsoidal surface intersects the rotation axis at two points; these two points define the minima of the time-averaged potential.

We load atoms into the double-well TAAP from a TOP using the following procedure. First, we prepare a sample

[1] In making the rotating wave approximation, the time dependence of the Rabi frequency is removed.

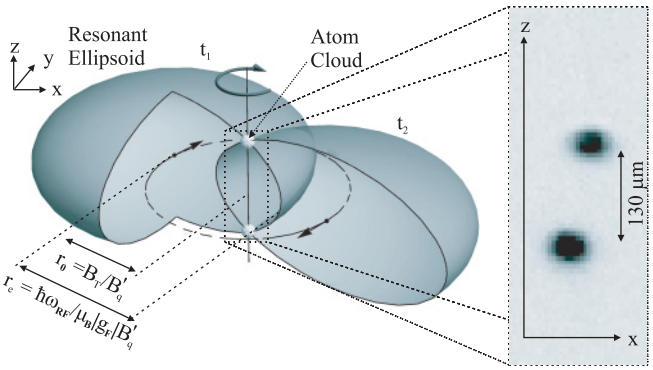

FIG. 1. (Color online) The instantaneous potential of the TAAP trap at two different times in the rotation cycle. The intersection of this potential with the rotation axis gives the minima of the TAAP at which the AP remains stationary. The inset shows an *in situ* absorption image of a thermal cloud trapped at these positions. We attribute the tilt evident in this image to a misalignment of the rotation axis with respect to the symmetry axis of the quadrupole potential.

of cold atoms in the TOP trap [see Fig. 2(a)]. The rf dressing field is then rapidly switched on while ensuring B_T satisfies the inequality $\omega_{rf} < |g_F \mu_B B_T/\hbar| < 2\omega_{rf}$ [Fig. 2(b)]. The lower bound ensures the atoms are loaded into the correct dressed state while the upper bound prevents higher harmonics of ω_{rf} from coming into resonance and causing unwanted evaporation. At this stage the modification of the time-averaged potential is minimal (the ellipsoids of Fig. 1 do not yet intersect with the rotation axis). Decreasing the TOP field to $\omega_{rf} = |g_F \mu_B B_T/\hbar|$ transfers the atoms onto the ellipsoidal shell [Fig. 2(c)]. A further decrease in the TOP field gives rise to a double-well potential in the z direction. Note that the atoms stay on resonance at *all* times in the TAAP trap. The well separation is given by the distance between the points of intersection of the ellipsoidal surface with the

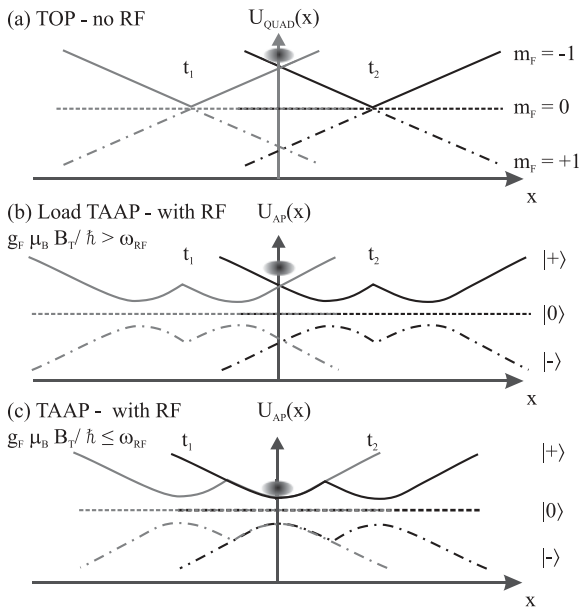

FIG. 2. The instantaneous potential of (a) the TOP, (b) the TAAP loading and (c) the TAAP potentials along the x axis at time t_1 in the rotation cycle and time t_2 half a period later.

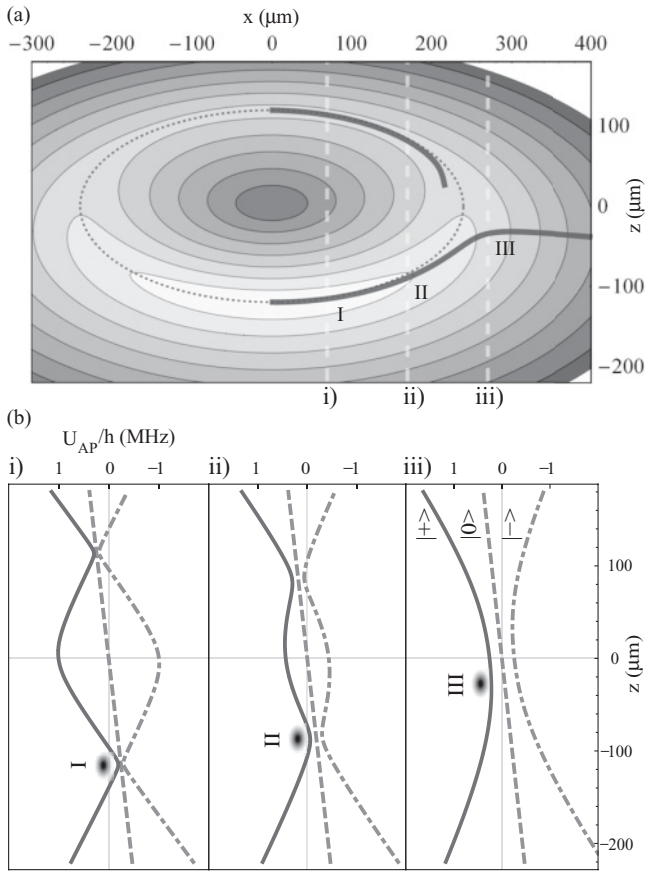

FIG. 3. (a) A contour plot of the AP in the xz plane for a gradient of $B'_q = 84$ G/cm and for linearly polarized rf with $B_{rf} = 0.5$ G. The dashed lines indicate the position of the rotation axis of the ellipsoid for different values of B_T. (b) The potential along these lines for the three dressed states. The slope in the potentials corresponds to the gravitational potential energy of a ^{87}Rb atom. Note the variation of the coupling at the atom's position.

rotation axis: a decrease in B_T moves the atom clouds further along the ellipsoid, thus increasing their separation. The TAAP potential in the z direction is that along the rotation axis of the ellipsoid as depicted in Fig. 3. The effect of the time averaging is to give confinement along the surface, thus preventing the atoms from spreading out over the ellipsoid.

Our TOP trap apparatus (with $\omega_T = 2\pi \times 7$ kHz) routinely produces BECs of 1×10^5 atoms of ^{87}Rb in the $|F = 1, m_F = -1\rangle$ hyperfine state. The rf dressing field is applied through coaxial coil pairs placed symmetrically about the trap center along the x, y, and z axes; this allows any arbitrary polarization but in these experiments it was either polarized circularly with $\mathbf{B}_{rf}(t)$ in the xy plane or linearly with $\mathbf{B}_{rf}(t) \propto \hat{\mathbf{e}}_\mathbf{z}$.

In Fig. 4 the vertical position of atoms in the lower well of the TAAP trap is plotted as a function of the magnitude of the rotating bias field B_T for two different quadrupole gradients. Here we apply linearly polarized rf along the z direction with $B_{rf} = 0.5$ G and $\omega_{rf} = 2\pi \times 1.4$ MHz. For these parameters the ellipsoidal surface touches the rotation axis when $B_T = 2$ G, at which stage the atoms are loaded into the TAAP trap. The polarization effects mentioned above and the gravitational sag of the atoms mean that as B_T is lowered the atoms do not

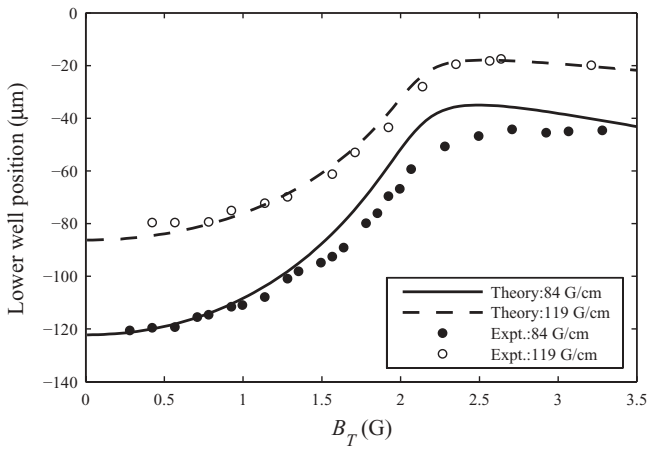

FIG. 4. Vertical displacement of the atoms from the static quadrupole field center in the lower well of the TAAP trap as a function of the magnitude of the rotating bias field B_T. This is plotted for two different field gradients, $B'_q = 84$ G/cm and $B'_q = 119$ G/cm.

follow the perfect ellipsoidal trajectory that one would expect from the idealized picture above. (In Fig. 3 compare the dotted ellipsoid to the actual position of the minima shown in black.)

It is evident in Fig. 3 that gravitational sag makes it impossible to load into the upper well for this quadrupole gradient (as denoted by the discontinuity in the black line in Fig. 3 indicating positions where there is no minimum in the upper half of the potential). This difficulty can be overcome by loading at higher gradients (230 G/cm) and lowering B_T to a final value of 1.7 G. A subsequent decrease in the gradient over ~400 ms (limited by speed of power supply) to 80 G/cm fully splits the cloud (see absorption image of Fig. 1). Using higher values for B_T during this loading procedure decreases the barrier height and prevents atoms from staying in the upper well. Lower values for B_T decrease the coupling at the potential minima and result in a lifetime insufficient to observe the separated clouds. The chosen values balance these competing effects.

In addition, the reduced lifetime explains why no data were taken in Fig. 4 for $B_T < 0.4$ G as the lifetime proved to be insufficient to make reliable measurements of the position. This effect is due to Landau-Zener (LZ) transitions to untrapped dressed states. The LZ transition probability for transitions between adjacent dressed states in the $F = 1$ manifold is given by [20]

$$P_{LZ}(\mathbf{r}) = 1 - \left[1 - \exp\left(-\frac{\pi\hbar\Omega_R^2(\mathbf{r})}{2g_F\mu_B B'_q v}\right)\right]^2, \qquad (4)$$

where v is the velocity of the atom through the avoided crossing. The lifetime of atoms in the TAAP trap, τ, varies as $\tau \propto 1/P_{LZ}(\mathbf{r}) + \tau_0$, where the offset τ_0 takes into account the finite extent of the cloud. Figure 5 shows the variation in trap lifetime for a TAAP dressed with linearly polarized rf. For this polarization, $\Omega_R(\mathbf{r})$ is a linear function of B_T and the lifetime changes by two orders of magnitude as B_T is ramped down. By choosing circularly polarized rf of the appropriate handedness, one can engineer a situation where the Rabi frequency increases as B_T is lowered. In this case

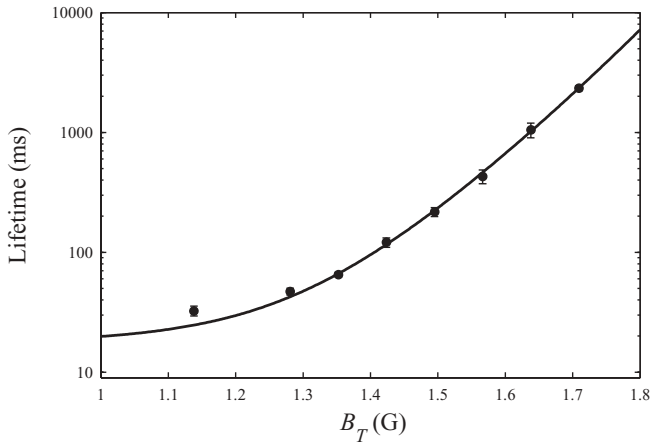

FIG. 5. The lifetime of atoms in the TAAP trap for linearly polarized rf with $B_{rf} = 0.5$ G and a radial quadrupole gradient of $B'_q = 84$ G/cm. For this polarization of rf, the $\Omega_R(\mathbf{r})$ varies linearly with B_T (see text for more details).

we apply rf fields in two directions, each with an amplitude of $B_{rf} = 0.5$ G. The predicted Rabi frequency $\Omega_R \sim 300$ kHz close to the south pole of the ellipsoidal surface agrees well with spectroscopy measurements of the trap bottom. These effects combine to give a lifetime of up to 10 s in the lower TAAP well. In addition, we have measured trapping frequencies as a function of B_T and observed good agreement with theoretical predictions, as shown in Fig. 6. In this trap we have successfully cooled a thermal cloud to quantum degeneracy. Starting with a sample of 1.5×10^6 atoms at ~0.7 μK in the TOP trap, we observe an atom loss of approximately one-third during the TAAP loading process with no substantial heating. The loss mechanism is attributed to increased LZ losses when the avoided crossing spirals through the cloud. A subsequent rf-evaporation sweep over 3 s with an additional weaker field (~0.05 G) cools the sample well below the critical temperature of 125 nK, creating a BEC of 5×10^4 atoms. For these frequency sweeps we have used transitions both

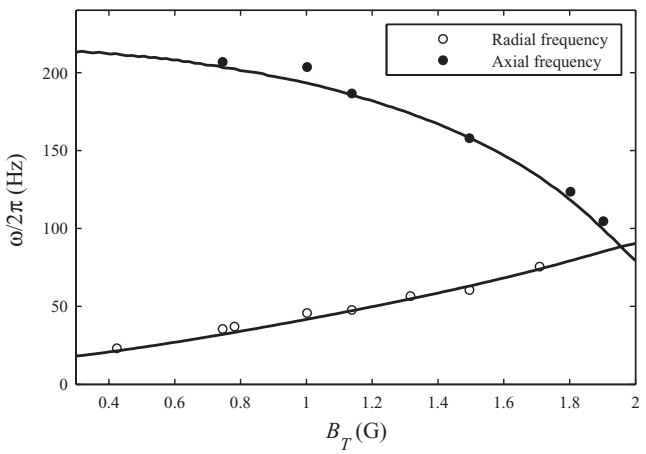

FIG. 6. Trapping frequencies of the atoms in the lower well of the TAAP trap as a function of the magnitude of the rotating field B_T. These frequencies are for a TAAP dressed with circularly polarized rf, $B_{rf} = 0.5$ G, and for $B'_q = 84$ G/cm.

within and beyond the rotating wave approximation and observed comparable efficiencies [16]. A BEC can be held in the TAAP trap without any evaporative rf for more than 3 s without any discernible heating.

In conclusion we have presented the realization of a time-averaged adiabatic potential which promises an accessible route to a large variety of purely magnetic trapping geometries with tunable parameters. The loading scheme presented above has acceptable losses and negligible heating. Furthermore, we show it is possible to evaporatively cool atoms to below quantum degeneracy in such a potential. Since completing the work presented above, we have successfully employed the TAAP trap as an intermediate stage for loading an rf dressed-state potential (lowering B_T to zero), which is of interest for studying low-dimensional physics [10].

This work has been supported by the Engineering and Physical Sciences Research Council under Grant No. EP/D000440.

[1] I. Lesanovsky and W. von Klitzing, Phys. Rev. Lett. **99**, 083001 (2007).
[2] M. H. Anderson, J. R. Ensher, M. R. Matthews, C. E. Wieman, and E. A. Cornell, Science **269**, 198 (1995).
[3] N. R. Thomas, A. C. Wilson, and C. J. Foot, Phys. Rev. A **65**, 063406 (2002).
[4] A. S. Arnold, C. S. Garvie, and E. Riis, Phys. Rev. A **73**, 041606(R) (2006).
[5] P. F. Griffin, E. Riis, and A. S. Arnold, Phys. Rev. A **77**, 051402(R) (2008).
[6] S. Gupta, K. W. Murch, K. L. Moore, T. P. Purdy, and D. M. Stamper-Kurn, Phys. Rev. Lett. **95**, 143201 (2005).
[7] P. Rudy, R. Ejnisman, A. Rahman, S. Lee, and N. Bigelow, Opt. Express **8**, 159 (2001).
[8] N. Friedman, L. Khaykovich, R. Ozeri, and N. Davidson, Phys. Rev. A **61**, 031403(R) (2000).
[9] K. Henderson, C. Ryu, C. MacCormick, and M. G. Boshier, New J. Phys. **11**, 043030 (2009).
[10] O. Zobay and B. M. Garraway, Phys. Rev. Lett. **86**, 1195 (2001).
[11] Y. Colombe, E. Knyazchyan, O. Morizot, B. Mercier, V. Lorent, and H. Perrin, Europhys. Lett. **67**, 593 (2004).
[12] M. White, H. Gao, M. Pasienski, and B. DeMarco, Phys. Rev. A **74**, 023616 (2006).
[13] O. Morizot, C. L. G. Alzar, P. E. Pottie, V. Lorent, and H. Perrin, J. Phys. B **40**, 4013 (2007).
[14] T. Schumm, S. Hofferberth, L. M. Andersson, S. Wildermuth, S. Groth, I. Bar-Joseph, J. Schmiedmayer, and P. Krüger, Nat. Phys. **1**, 57 (2005).
[15] S. Hofferberth, I. Lesanovsky, B. Fischer, J. Verdu, and J. Schmiedmayer, Nat. Phys. **2**, 710 (2006).
[16] S. Hofferberth, B. Fischer, T. Schumm, J. Schmiedmayer, and I. Lesanovsky, Phys. Rev. A **76**, 013401 (2007).
[17] I. Lesanovsky, T. Schumm, S. Hofferberth, L. M. Andersson, P. Krüger, and J. Schmiedmayer, Phys. Rev. A **73**, 033619 (2006).
[18] I. Lesanovsky, S. Hofferberth, J. Schmiedmayer, and P. Schmelcher, Phys. Rev. A **74**, 033619 (2006).
[19] C. Cohen-Tannoudji, J. Dupont-Roc, and G. Grynberg, *Atom-Photon Interactions* (Wiley, 1992).
[20] N. V. Vitanov and K. A. Suominen, Phys. Rev. A **56**, R4377 (1997).